THE JOURNAL OF PHYSICAL CHEMISTRY C

Article

Cite This: J. Phys. Chem. C 2019, 123, 11539−11545

pubs.acs.org/JPCC

C−C Coupling Reactions Catalyzed by Gold Nanoparticles: Evidence for Substrate-Mediated Leaching of Surface Atoms Using Localized Surface Plasmon Resonance Spectroscopy

Farshid Mohammadparast,[⊥] Andishaeh P. Dadgar,[⊥] Ravi Teja A. Tirumala,[⊥] Sayeed Mohammad,[⊥] C. Ozge Topal,[∥] A. Kaan Kalkan,[∥] and Marimuthu Andiappan*[,⊥]

[⊥]School of Chemical Engineering and [∥]School of Mechanical and Aerospace Engineering, Oklahoma State University, Stillwater, Oklahoma 74078, United States

Supporting Information

ABSTRACT: Heterogeneous metal nanocatalysts have recently emerged as attractive catalysts for a variety of couplings (e.g., C−C, C−N, C−S, C−O, etc.). However, the characterization of the catalytic pathway remains challenging. By exploiting localized surface plasmon resonance (LSPR) of the catalytically relevant gold (Au) nanostructure, we show that UV−vis spectroscopy can be used to confirm the homogeneous catalytic pathway. Specifically, we have demonstrated that Au nanoparticles under C−C coupling conditions undergo substrate-induced leaching to form homogeneous Au catalytic species. The LSPR spectroscopic approach opens a new door to track stability of nanocatalysts and characterize the catalytic pathway in a range of coupling reactions.

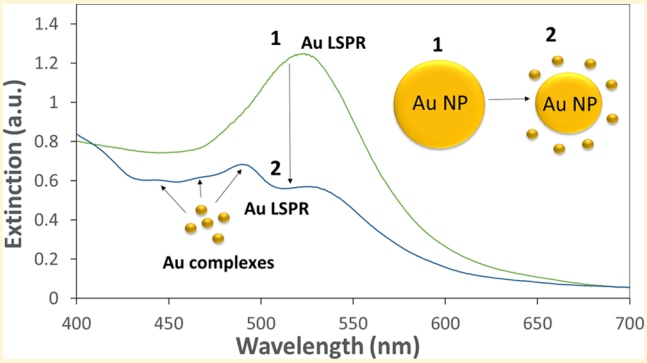

INTRODUCTION

Metal-catalyzed coupling reactions (MCCRs) have found widespread application in premier organic synthesis from pharmaceutical compounds to polymers.[1,2] MCCRs have been traditionally carried out by homogeneous Pd-complexed catalysts.[1,3] However, Pd and most of the ligands associated with the homogeneous catalysts are toxic. Therefore, conventional homogeneous Pd-catalyzed processes typically require several expensive downstream unit operations to reduce the metal residue below the maximum allowable level in the final product (e.g., active pharmaceutical ingredient, API).[4−6] In recent years, heterogeneous metal nanocatalysts have emerged as high-performance alternatives to conventional homogeneous complexes to drive coupling reactions.[2,7−29] For example, nanocatalysts built on Au, Cu, Pd, and their alloys can drive a variety of couplings (e.g., C−C, C−N, C−S, C−O, etc.) and exhibit excellent yield, catalytic activity, and broad substrate scope.[7−15,30−38] These catalysts do not require ligands and are in general not sensitive to air and moisture. They have the potential to reduce the need for expensive downstream operations for separating the metal catalyst from the final product (e.g., API).

While recent years have witnessed a growing demand for nanocatalysts, there is also a continuing controversy whether the catalysis occurs on the surface of nanoparticles (i.e., heterogeneous pathway) or on leached metal ions in solution (i.e., homogeneous pathway). Therefore, characterization of the catalytic pathway and determination of nanocatalyst stability under relevant reaction conditions remain ongoing challenges within the field.[7−15,30−38] The leaching of surface atoms into solvent can depend on the reaction temperature, size of the nanoparticle, nature of the solvent, substrate, base, and stabilizer.[30,39] A common leaching test used to determine nanocatalyst stability mainly employs filtration. This test involves post-catalytic analysis of the leached metal atoms in the filtered supernatant reaction solution using techniques such as inductively coupled plasma mass spectrometry (ICP-MS) and characterization of the spent nanocatalyst using transmission electron microscopy (TEM). This test has several drawbacks; for example, it has been reported that the leached metal atoms can redeposit quickly onto the catalyst during filtration and may not be detected in the supernatant solution.[31]

Herein, for coupling reaction involving Au nanoparticles, we propose an alternative method that is based on localized surface plasmon resonance (LSPR). LSPR of metal nanoparticles can conveniently be monitored by ultraviolet−visible (UV−vis) light extinction spectroscopy.[40−44] Specifically, the LSPR spectrum of metal nanoparticles of a given average size is characterized by a certain extinction intensity, peak wavelength, and full width at half-maximum. Therefore, when the nanoparticles undergo leaching of surface atoms, changes in

Received: December 26, 2018
Revised: March 29, 2019
Published: April 1, 2019

Downloaded via OKLAHOMA STATE UNIV STILLWATER on September 27, 2019 at 05:50:39 (UTC).
See https://pubs.acs.org/sharingguidelines for options on how to legitimately share published articles.

© 2019 American Chemical Society

DOI: 10.1021/acs.jpcc.8b12453
J. Phys. Chem. C 2019, 123, 11539−11545

these characteristics can be exploited to trace the change in the average size of the nanoparticles (for more details, see the Supporting Information).[45]

EXPERIMENTAL METHODS

Representative Procedure for Coupling Reaction. In the present work, we investigated the C−C coupling reaction catalyzed by Au nanoparticles. Specifically, the homocoupling of phenylacetylene (PA) was selected as a model reaction. The reaction was carried out on a magnetic hot plate with an aluminum reaction block around a 200 mL three-necked round bottom flask. To control temperature, a thermocouple was connected to the hot plate and submerged in the reactor. As a first step in the reaction procedure, Au nanoparticles dispersed in water was heated to 85 °C in a three-necked round bottom flask. Twenty-four milliliters of DMF was then added to this Au nanoparticle suspension. After the addition of DMF to Au nanoparticle suspension, the composition of the solvent mixture in the RBF was an 83%/17% v/v mixture of water/DMF. Two grams of potassium carbonate was then added under stirring. Two milliliters of phenylacetylene (18.2 mmol) was finally added to this mixture at 85 °C to start the reaction. UV−vis extinction spectra were acquired using an Agilent Cary 60 spectrophotometer. In operando measurements were taken using a dip probe accessory and a fiber optic coupler with a stainless steel tip. The reaction solution was also characterized using GC−MS (Shimadzu QP2010S), TEM, and HR-ESI-MS. TEM images of the reaction samples were taken using a JEOL JEM-2100. HR-ESI-MS spectra of the reaction samples were collected on an LTQ Orbitrap system with an ESI source (for more details, see the Supporting Information).[45]

RESULTS AND DISCUSSION

The homocoupling reaction of PA was carried out at 85 °C using potassium carbonate (K_2CO_3) and 83/17 (volumetric ratio) mixture of water/dimethylformamide (DMF) as the base and solvent, respectively. Samples of reaction mixture were taken at frequent time intervals for UV−vis extinction spectra measurements and TEM imaging. In Figure 1, we show the UV−vis extinction spectra of the reaction mixture measured before the addition of the substrate (i.e., PA) and at different reaction times. We also show the representative and complete deconvoluted extinction spectra in Figure 2 and Figure S5, respectively. As seen from Figure 2 and Figure S5, the extinction acquired before the addition of phenylacetylene shows mainly the LSPR peak after baseline (mainly interband absorption in Au) subtraction.[45] Upon addition of phenylacetylene, the LSPR peak is attenuated along with the appearance of new peaks in the 400−500 nm region. It has been shown that organometallic complexes of noble metals exhibit absorption peaks in this region.[46,47] After PA addition, the LSPR peak of Au nanoparticles also red-shifts slightly as seen from Figure 1. This adsorbate-induced red-shift in the LSPR peak position is due to the expected adsorbate-induced change in the dielectric constant of the surrounding medium.[44,48] The decrease in LSPR extinction and the appearance of new extinction peaks in the 400−500 nm region suggest that the phenylacetylene is inducing a leaching process from the surface of the Au nanoparticles forming soluble Au complexes in the reaction solution. It is worth mentioning here that the leaching of Au nanoparticles has also been confirmed in the literature using other spectroscopic techniques such as inductively coupled plasma mass spectrometry and X-ray photoelectron spectroscopy for similar reaction conditions in Au-nanoparticle-catalyzed Sonogashira coupling between phenylacetylene and iodobenzene.[30] It could be argued that the changes observed in the UV−vis extinction spectra may be due to Au nanoparticle aggregate formation. However, when there is aggregate formation, an additional lower-energy LSPR peak is expected for Au aggregates. Since the UV−vis extinction spectra in Figure 1 do not show any such features, we rule out any significant aggregation formation.[49]

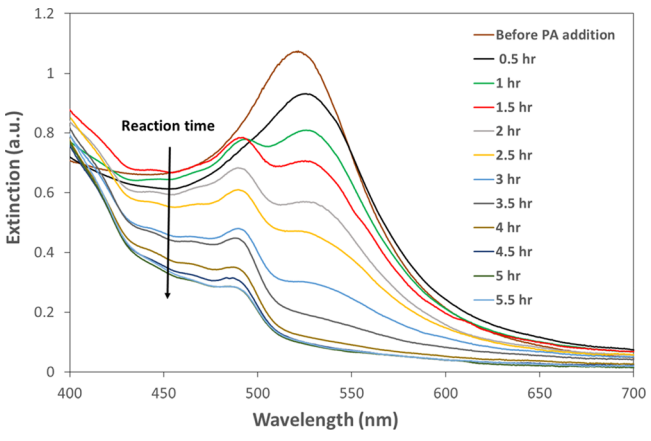

Figure 1. UV−vis extinction spectra of reaction mixture measured before the addition of phenylacetylene (PA, 0 h) and at different reaction times during homocoupling of phenylacetylene.

We also verified that the reactant (i.e., PA) and the expected homocoupling product (diphenyldiacetylene (DPDA)) exhibit absorption peaks only in the 200−350 nm region and do not exhibit any absorption features in the 400−500 nm region (e.g., see Figure S2).[45,50] Therefore, the new extinction peaks observed in the 400−500 nm region are most likely due to the different Au homogeneous catalytic species that participate in the homogeneous catalytic cycle. As seen from Figure 2d and Figure S5, the deconvoluted extinction spectra show up to five extinction peaks due to the homogeneous Au catalytic species at peak wavelengths of 403, 416, 445, 470, and 492 nm, along with the LSPR peak of Au nanoparticles at 528 nm. It is worth mentioning here that a combination of two (or more) of these extinction peaks may correspond to a single homogeneous Au species. For example, it has been reported that homogeneous copper-phenylacetylide complex (Cu-PA) exhibits two absorption peaks with peak wavelengths of ∼390 and 476 nm.[46,47] Also, in Figure 2f, we show the intensity of the five extinction peaks as a function of reaction time. These plots basically provide qualitative trends for kinetics of homogeneous Au catalytic species concentrations. As seen from Figure 2f, the concentrations of Au catalytic species exhibit maxima at 2 h of reaction followed by a decreasing trend. It has been shown that the in situ generated homogeneous palladium catalytic species can undergo decomposition to form palladium black when the concentration of stabilizing species such as ligand or reactant concentration is low.[4,8,51−53] As such, we attribute the decreasing trends in Figure 2f to the expected decomposition of the homogeneous Au catalytic species with the decreasing concentration of PA.

To identify the soluble Au complexes present in the reaction solution, we performed high-resolution electrospray ionization mass spectrometry (HR-ESI-MS) on the supernatant solution

DOI: 10.1021/acs.jpcc.8b12453
J. Phys. Chem. C 2019, 123, 11539−11545

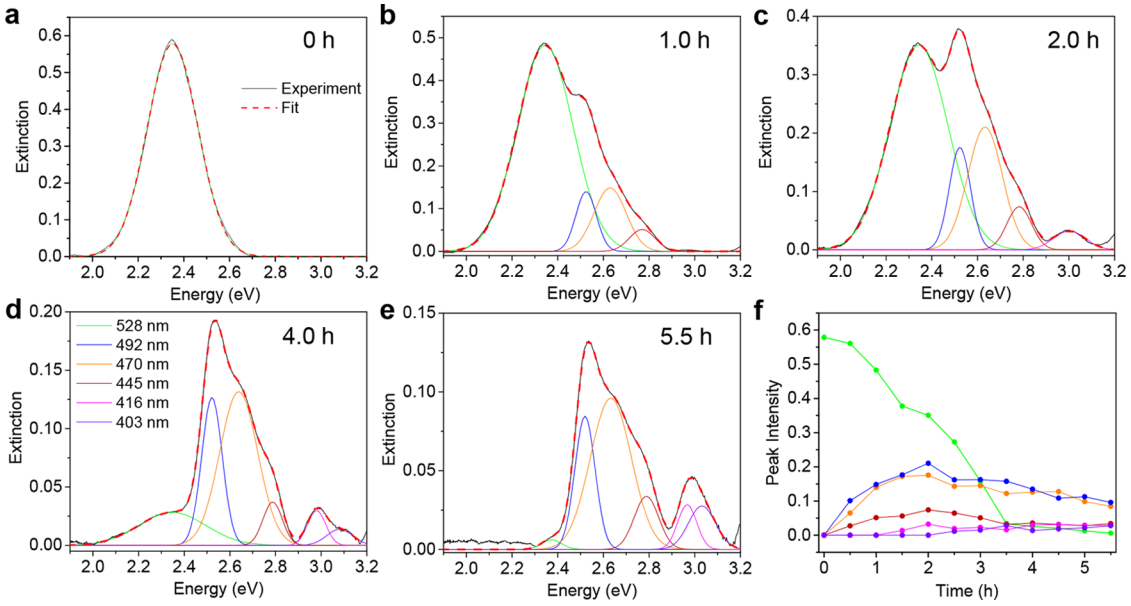

Figure 2. (a–e) Deconvoluted extinction spectra of Au nanoparticles after the addition of PA at 0, 1, 2, 4, and 5.5 h. The spectra are baseline-corrected and fit to Gaussians, which are coded with different colors. Representative peak positions of the deconvoluted peaks are given for (d) 4.0 h. (f) Time evolution of the peak intensities at 0.5 h intervals. Colors are as in panels (a–e).

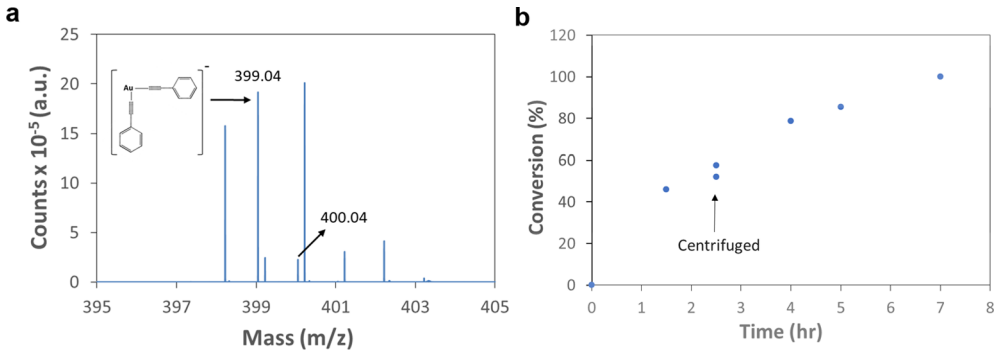

Figure 3. (a) Representative HR-ESI-MS spectrum of supernatant solution of reaction mixture taken from Au-nanoparticle-catalyzed homocoupling of phenylacetylene. (b) Reaction conversion as a function of reaction time for the homocoupling of phenylacetylene.

of reaction solution. In the HR-ESI-MS spectrum (Figure 3a), we observe seven negative ions in the m/z range of 400. Five of these ions have a fractional mass of 0.22, and the other two ions (with m/z = 399.04 and 400.04) have a fractional mass of 0.04. These fractional masses indicate that these ions are derived from two different compounds. Since the ions with a fractional mass of 0.22 give an isotope distribution inconsistent with gold's single isotope, we disregard them for further consideration. The ions with a fractional mass of 0.04 give an isotope distribution consistent with that predicted for the $[Au(PA)_2]^-$ compound, and the mass error for the predicted compound is less than 5 ppm.[45] We have also analyzed the reaction samples with gas chromatography–mass spectrometry (GC–MS) and confirmed the presence of the homocoupling product DPDA in the solution (see Figure S3).[45] The leaching of Au nanoparticles and the presence of a homogenous Au species (Figures 1–3b) confirm the homogeneous catalytic pathway contribution for the homocoupling of phenylacetylene (PA) investigated in this study. Although these results confirm the contribution of the homogeneous catalytic pathway in Au-nanoparticle-mediated C–C coupling of PA, we do not rule out the possible heterogeneous pathway that can happen in parallel.

To further support our conclusions that Au complexes can catalyze the homocoupling reaction, we carried out the reaction using the supernatant solution containing homogeneous Au complexes as the only catalytic species. The homocoupling reaction of PA was first carried out using Au nanoparticles, and reaction progress was monitored using GC–MS. DPDA was observed as the only product of the homocoupling of PA. When the PA conversion was ~52%, the reaction was stopped and Au nanoparticles were removed from the reaction solution using centrifugation. The reaction was then allowed to continue, and PA conversion was monitored in the supernatant solution containing homogeneous Au complexes. Figure 3b shows PA conversion observed as a function of reaction time from this experiment. The results shown in Figure 3b confirm that the homogeneous Au complexes can indeed catalyze the homocoupling reaction to 100% conversion.

To test the applicability of LSPR spectroscopy to predict the average size of Au nanoparticles in the reaction samples, the samples collected after 1, 1.5, 2, and 2.5 h of reaction were

DOI: 10.1021/acs.jpcc.8b12453
J. Phys. Chem. C 2019, 123, 11539–11545

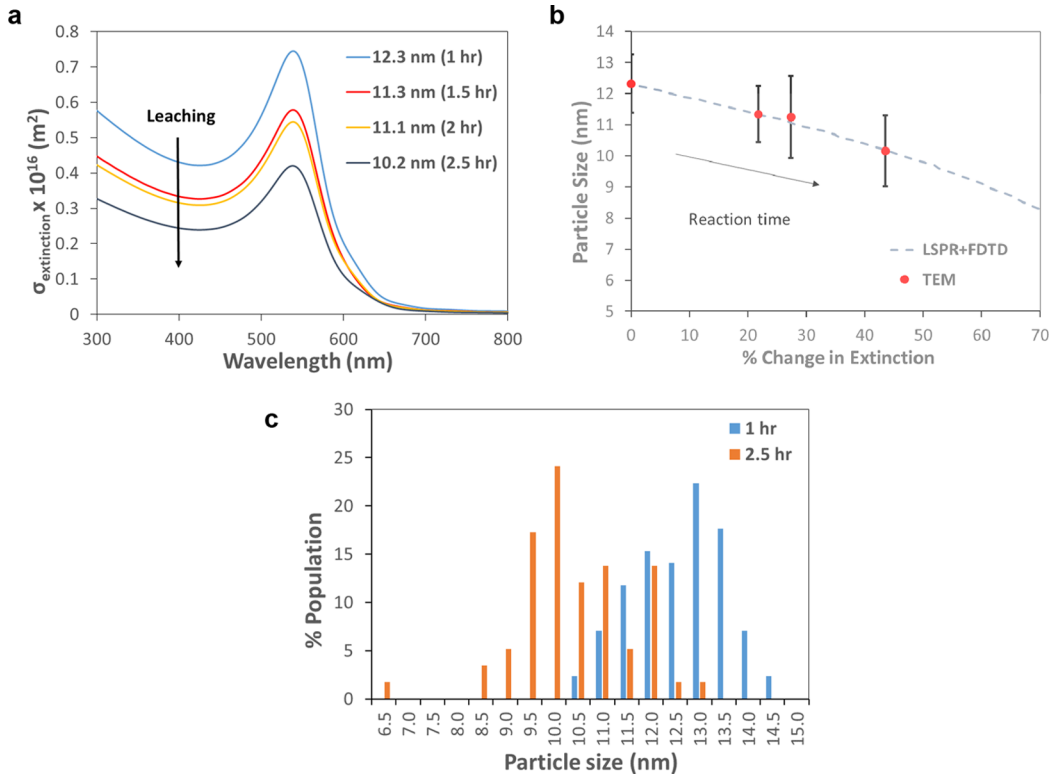

Figure 4. (a) Simulated LSPR responses for the leaching of Au spherical nanoparticles. The legend shows the reaction time and the predicted average size of Au nanoparticles in the respective reaction sample. (b) Average size of Au nanoparticles predicted from LSPR responses and FDTD simulations for different reaction samples as a function of % change in extinction intensity of the respective samples at LSPR peak wavelength. For comparison, TEM-measured average sizes of Au nanoparticles are also shown. (c) Size distributions of Au nanoparticles measured from TEM images for the reaction samples collected after 1 and 2.5 h of C−C homocoupling reaction.

characterized using TEM to determine the average size of nanoparticles, and the deconvoluted LSPR peaks of the respective Au nanoparticle samples were matched with finite-difference time-domain (FDTD) simulations. We utilized a reliable and widely used Lumerical FDTD program to perform FDTD simulations.[54,55] The built-in material model in the program Au-Palik was used for the optical constants of Au. This material model in the program is based on the experimental data (real and imaginary parts of the refractive index at different wavelengths), rather than on an analytical model. For the experimental data, the program uses the real and imaginary parts of the refractive index values taken from the Palik handbook.[56] The simulation procedures are described in detail in the Supporting Information.[45]

Figure 4a shows the simulated extinction spectra that are matched with LSPR spectra of Au nanoparticles. In Figure 4b, we show the comparison between Au nanoparticle sizes predicted from LSPR responses and average nanoparticle sizes measured from TEM for different reaction samples collected as a function of reaction time. As seen from Figure 4b, the LSPR-predicted and TEM-measured average sizes match well. We also show in Figure 4c the representative particle size distributions measured from TEM for the reaction samples collected after 1.0 and 2.5 h of reaction. The decreasing trend in average particle size in Figure 4b along with the shift in particle size distribution toward smaller sizes in Figure 4c further confirms the leaching of Au nanoparticles during the homocoupling reaction.

We also investigated the applicability of LSPR spectroscopy for nanoparticle growth systems. For this system, we selected the growth of spherical Au nanoparticles using a seeded growth approach.[57] In this approach, we prepared quasispherical Au nanoparticles (average size = 8.0 nm and standard deviation in size distribution = 0.6 nm) and used those as seeds for growth. Figure 5a shows the representative TEM image of seed nanoparticles. In Figure S1, we also show the representative TEM image of larger nanoparticles obtained at the end of the growth process. For the growth of larger nanoparticles, a known amount of growth solution comprising the gold precursor was added gradually to the seed solution. For each addition, in operando UV−vis extinction spectra measurements were made and TEM samples were taken to determine the LSPR response and average size of nanoparticles, respectively. Figure 5b shows the in operando extinction spectra of Au nanoparticles measured during this growth process. Figure 5c shows the representative particle size distributions measured from TEM for the seed and larger Au nanoparticles obtained at the end of the growth process. In operando LSPR responses acquired for each addition during the growth process were matched with FDTD-simulated results to predict Au nanoparticle size for each growth step.[45] The comparison between nanoparticle sizes predicted from in operando LSPR responses and average nanoparticle sizes measured from TEM is shown in Figure 5d. The shift in particle size distribution toward larger sizes in Figure 5c along with the increasing trend in average particle size in Figure 5d confirms the growth of Au nanoparticles. Figure 5d shows that there is also a consistency between TEM analysis and the LSPR spectral changes for seeded growth of the particles.

DOI: 10.1021/acs.jpcc.8b12453
J. Phys. Chem. C 2019, 123, 11539−11545

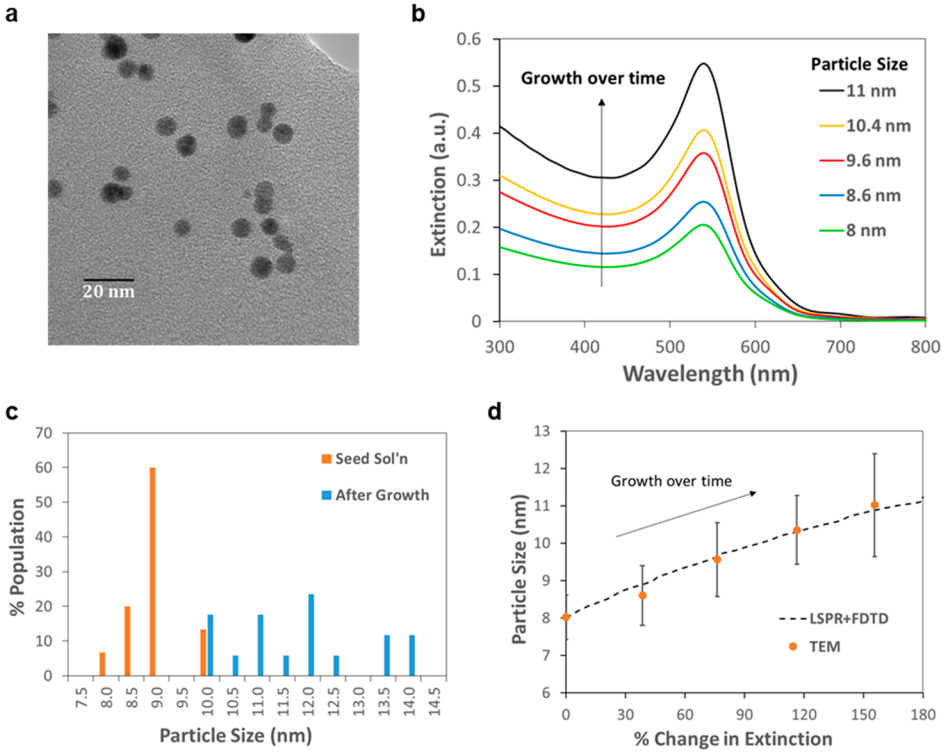

Figure 5. (a) Representative TEM image of spherical Au nanoparticles used as seeds for growth. (b) In operando UV−vis extinction spectra that show LSPR responses for growth of Au spherical nanoparticles from seed nanoparticles of 8.0 nm average diameter. The legend shows the predicted average size of Au nanoparticles in the respective samples. (c) TEM-measured size distributions of seed and larger Au nanoparticles obtained at the end of growth process. (d) Average size of Au nanoparticles predicted from LSPR responses and FDTD simulations for each growth step as a function of % change in extinction intensity at LSPR peak wavelength. For comparison, TEM-measured average sizes of Au nanoparticles are also shown.

CONCLUSIONS

For the selected C−C coupling reaction, we have shown that Au nanoparticles serve as precursors for the in situ formation of homogeneous Au catalytic species. Specifically, using the changes observed in UV−vis extinction spectra, we have shown that Au nanoparticles undergo substrate (i.e., PA)-induced leaching under C−C coupling reaction conditions. We have also confirmed the presence of the homogeneous Au complex in the reaction solution using HR-ESI-MS. In summary, we have demonstrated that the homogeneous catalytic pathway can occur in Au-nanoparticle-mediated C−C coupling reaction of PA, in addition to the possible heterogeneous pathway.

ASSOCIATED CONTENT

Supporting Information

The Supporting Information is available free of charge on the ACS Publications website at DOI: 10.1021/acs.jpcc.8b12453.

Detailed synthesis methods, experimental and characterization procedures, finite-difference time-domain (FDTD) simulation procedures, monolayer calculations (PDF)

AUTHOR INFORMATION

Corresponding Author

*E-mail: mari.andiappan@okstate.edu.

ORCID

A. Kaan Kalkan: 0000-0001-5878-3413

Marimuthu Andiappan: 0000-0002-4211-030X

Author Contributions

F.M. and A.P.D. contributed equally. F.M., A.P.D., R.T.A.T., and M.A. developed the project and analyzed the results. F.M. and A.P.D. performed the experiments and simulations. S.M. and A.K.K. helped with analysis. C.O.T. performed the deconvolution of the UV−vis extinction peaks. M.A. is the M.S. and Ph.D. adviser of A.P.D., F.M., and R.T.A.T.; A.K.K. is the Ph.D. adviser of C.O.T. The manuscript was written by M.A. and A.P.D. with minor contributions from A.K.K.

Notes

The authors declare no competing financial interest.

ACKNOWLEDGMENTS

The research results discussed in this publication were made possible in part by funding through the award for project number HR18-093 from the Oklahoma Center for the Advancement of Science and Technology. Additionally, A.K.K. acknowledges the funding by National Science Foundation (Award #1707008). The TEM images were acquired at the Oklahoma State University (OSU) Microscopy Laboratory. HR-ESI-MS spectra were acquired at the OSU DNA and Protein Core Facility. We are grateful to Dr. Steven Hartson for his assistance with HR-ESI-MS data analysis. We also thank Dr. Jeffrey L. White, Dr. R. Russell Rhinehart, and Dr. Toby Nelson for suggestions and comments on the manuscript.

REFERENCES

(1) Diederich, F.; Stang, P. J. *Metal-Catalyzed Cross-Coupling Reactions*; John Wiley & Sons, 2008.

DOI: 10.1021/acs.jpcc.8b12453
J. Phys. Chem. C 2019, 123, 11539−11545

(2) Evano, G.; Blanchard, N. *Copper-Mediated Cross-Coupling Reactions*, 1 edition.; Wiley: Hoboken, New Jersey, 2013.
(3) Jana, R.; Pathak, T. P.; Sigman, M. S. Advances in Transition Metal (Pd,Ni,Fe)-Catalyzed Cross-Coupling Reactions Using Alkyl-Organometallics as Reaction Partners. *Chem. Rev.* **2011**, *111*, 1417−1492.
(4) Merritt, J. M.; Andiappan, M.; Pietz, M. A.; Richey, R. N.; Sullivan, K. A.; Kjell, D. P. Mitigating the Risk of Coprecipitation of Pinacol during Isolation from Telescoped Miyaura Borylation and Suzuki Couplings Utilizing Boron Pinacol Esters: Use of Modeling for Process Design. *Org. Process Res. Dev.* **2016**, *20*, 178−188.
(5) Cooper, T. W. J.; Campbell, I. B.; Macdonald, S. J. F. Factors Determining the Selection of Organic Reactions by Medicinal Chemists and the Use of These Reactions in Arrays (Small Focused Libraries). *Angew. Chem. Int. Ed.* **2010**, *49*, 8082−8091.
(6) *Q3D Elemental Impurities - Guidance for Industry* https://www.fda.gov/downloads/drugs/guidances/ucm371025.pdf (accessed Jul 30, 2017).
(7) Farina, V. High-Turnover Palladium Catalysts in Cross-Coupling and Heck Chemistry: A Critical Overview. *Adv. Synth. Catal.* **2004**, *346*, 1553−1582.
(8) Phan, N. T.; Van Der Sluys, M.; Jones, C. W. On the Nature of the Active Species in Palladium Catalyzed Mizoroki−Heck and Suzuki−Miyaura Couplings − Homogeneous or Heterogeneous Catalysis, A Critical Review. *Adv. Synth. Catal.* **2006**, *348*, 609−679.
(9) Balanta, A.; Godard, C.; Claver, C. Pd Nanoparticles for C−C Coupling Reactions. *Chem. Soc. Rev.* **2011**, *40*, 4973−4985.
(10) Peiris, S.; Sarina, S.; Han, C.; Xiao, Q.; Zhu, H.-Y. Silver and Palladium Alloy Nanoparticle Catalysts: Reductive Coupling of Nitrobenzene through Light Irradiation. *Dalton Trans.* **2017**, *46*, 10665−10672.
(11) Xiao, Q.; Sarina, S.; Bo, A.; Jia, J.; Liu, H.; Arnold, D. P.; Huang, Y.; Wu, H.; Zhu, H. Visible Light-Driven Cross-Coupling Reactions at Lower Temperatures Using a Photocatalyst of Palladium and Gold Alloy Nanoparticles. *ACS Catal.* **2014**, *4*, 1725−1734.
(12) Hutchings, G. *Nanocatalysis: Synthesis and Applications*, 1 edition.; Polshettiwar, V., Asefa, T., Eds.; Wiley, 2013.
(13) Garcia, P.; Malacria, M.; Aubert, C.; Gandon, V.; Fensterbank, L. Gold-Catalyzed Cross-Couplings: New Opportunities for C-C Bond Formation. *ChemCatChem* **2010**, *2*, 493−497.
(14) Molnar, A. Efficient, Selective, and Recyclable Palladium Catalysts in Carbon-Carbon Coupling Reactions. *Chem. Rev.* **2011**, *111*, 2251−2320.
(15) Maria Thomas, A.; Sujatha, A.; Anilkumar, G. Recent Advances and Perspectives in Copper-Catalyzed Sonogashira Coupling Reactions. *RSC Adv.* **2014**, *4*, 21688−21698.
(16) Boronat, M.; Combita, D.; Concepción, P.; Corma, A.; García, H.; Juárez, R.; Laursen, S.; de Dios López-Castro, J. Making C−C Bonds with Gold: Identification of Selective Gold Sites for Homo- and Cross-Coupling Reactions between Iodobenzene and Alkynes. *J. Phys. Chem. C* **2012**, *116*, 24855−24867.
(17) Li, Y.; El-Sayed, M. A. The Effect of Stabilizers on the Catalytic Activity and Stability of Pd Colloidal Nanoparticles in the Suzuki Reactions in Aqueous Solution†. *J. Phys. Chem. B* **2001**, *105*, 8938−8943.
(18) Pérez-Lorenzo, M. Palladium Nanoparticles as Efficient Catalysts for Suzuki Cross-Coupling Reactions. *J. Phys. Chem. Lett.* **2012**, *3*, 167−174.
(19) Feng, L.; Chong, H.; Li, P.; Xiang, J.; Fu, F.; Yang, S.; Yu, H.; Sheng, H.; Zhu, M. Pd−Ni Alloy Nanoparticles as Effective Catalysts for Miyaura−Heck Coupling Reactions. *J. Phys. Chem. C* **2015**, *119*, 11511−11515.
(20) Narayanan, R.; El-Sayed, M. A. Effect of Colloidal Catalysis on the Nanoparticle Size Distribution: Dendrimer−Pd vs PVP−Pd Nanoparticles Catalyzing the Suzuki Coupling Reaction. *J. Phys. Chem. B* **2004**, *108*, 8572−8580.
(21) Zhu, M.; Diao, G. Magnetically Recyclable Pd Nanoparticles Immobilized on Magnetic Fe3O4@C Nanocomposites: Preparation, Characterization, and Their Catalytic Activity toward Suzuki and Heck Coupling Reactions. *J. Phys. Chem. C* **2011**, *115*, 24743−24749.
(22) Pd(0) Nanoparticles Supported Organofunctionalized Clay Driving C−C Coupling Reactions under Benign Conditions through a Pd(0)/Pd(II) Redox Interplay - *The Journal of Physical Chemistry C* (ACS Publications) https://pubs.acs.org/doi/10.1021/jp410709n (accessed Feb 13, 2019).
(23) Facile Deposition of Pd Nanoparticles on Carbon Nanotube Microparticles and Their Catalytic Activity for Suzuki Coupling Reactions - *The Journal of Physical Chemistry C* (ACS Publications) https://pubs.acs.org/doi/10.1021/jp800610q (accessed Feb 13, 2019).
(24) Park, J. C.; Heo, E.; Kim, A.; Kim, M.; Park, K. H.; Song, H. Extremely Active Pd@pSiO2Yolk−Shell Nanocatalysts for Suzuki Coupling Reactions of Aryl Halides. *J. Phys. Chem. C* **2011**, *115*, 15772−15777.
(25) Karousis, N.; Tsotsou, G.-E.; Evangelista, F.; Rudolf, P.; Ragoussis, N.; Tagmatarchis, N. Carbon Nanotubes Decorated with Palladium Nanoparticles: Synthesis, Characterization, and Catalytic Activity. *J. Phys. Chem. C* **2008**, *112*, 13463−13469.
(26) Understanding the Biosynthesis and Catalytic Activity of Pd, Pt, and Ag Nanoparticles in Hydrogenation and Suzuki Coupling Reactions at the Nano−Bio Interface - *The Journal of Physical Chemistry C* (ACS Publications) https://pubs.acs.org/doi/10.1021/jp508211t (accessed Feb 13, 2019).
(27) Jang, Y.; Chung, J.; Kim, S.; Jun, S. W.; Kim, B. H.; Lee, D. W.; Kim, B. M.; Hyeon, T. Simple Synthesis of Pd−Fe3O4 Heterodimer Nanocrystals and Their Application as a Magnetically Recyclable Catalyst for Suzuki Cross-Coupling Reactions. *Phys. Chem. Chem. Phys.* **2011**, *13*, 2512−2516.
(28) Pachón, L. D.; Thathagar, M. B.; Hartl, F.; Rothenberg, G. Palladium-Coated Nickel Nanoclusters: New Hiyama Cross-Coupling Catalysts. *Phys. Chem. Chem. Phys.* **2006**, *8*, 151−157.
(29) Jia, C.-J.; Schüth, F. Colloidal Metal Nanoparticles as a Component of Designed Catalyst. *Phys. Chem. Chem. Phys.* **2011**, *13*, 2457−2487.
(30) Kyriakou, G.; Beaumont, S. K.; Humphrey, S. M.; Antonetti, C.; Lambert, R. M. Sonogashira Coupling Catalyzed by Gold Nanoparticles: Does Homogeneous or Heterogeneous Catalysis Dominate? *ChemCatChem* **2010**, *2*, 1444−1449.
(31) Widegren, J. A.; Finke, R. G. A Review of the Problem of Distinguishing True Homogeneous Catalysis from Soluble or Other Metal-Particle Heterogeneous Catalysis under Reducing Conditions. *J. Mol. Catal. A: Chem.* **2003**, *198*, 317−341.
(32) Biffis, A.; Zecca, M.; Basato, M. Metallic Palladium in the Heck Reaction: Active Catalyst or Convenient Precursor? *Eur. J. Inorg. Chem.* **2001**, *2001*, 1131−1133.
(33) Schmidt, A. F.; Al-Halaiqa, A.; Smirnov, V. V. New Approaches to Heck Reaction Testing for Homogeneity-Heterogeneity. *Kinet. Catal.* **2008**, *49*, 395−400 S0023158408030129 .
(34) Ellis, P. J.; Fairlamb, I. J.; Hackett, S. F.; Wilson, K.; Lee, A. F. Evidence for the Surface-Catalyzed Suzuki−Miyaura Reaction over Palladium Nanoparticles: An Operando XAS Study. *Angew. Chem. Int. Ed.* **2010**, *49*, 1820−1824.
(35) Song, H. M.; Moosa, B. A.; Khashab, N. M. Water-Dispersable Hybrid Au−Pd Nanoparticles as Catalysts in Ethanol Oxidation, Aqueous Phase Suzuki−Miyaura and Heck Reactions. *J. Mater. Chem.* **2012**, *22*, 15953−15959.
(36) Fang, P. P.; Jutand, A.; Tian, Z. Q.; Amatore, C. Au−Pd Core−Shell Nanoparticles Catalyze Suzuki−Miyaura Reactions in Water through Pd Leaching. *Angew. Chem. Int. Ed.* **2011**, *50*, 12184−12188.
(37) Elias, W. C.; Signori, A. M.; Zaramello, L.; Albuquerque, B. L.; de Oliveira, D. C.; Domingos, J. B. Mechanism of a Suzuki-Type Homocoupling Reaction Catalyzed by Palladium Nanocubes. *ACS Catal.* **2017**, *7*, 1462−1469.
(38) Collins, G.; Schmidt, M.; O'Dwyer, C.; Holmes, J. D.; McGlacken, G. P. The Origin of Shape Sensitivity in Palladium-Catalyzed Suzuki−Miyaura Cross Coupling Reactions. *Angew. Chem. Int. Ed.* **2014**, *53*, 4142−4145.

DOI: 10.1021/acs.jpcc.8b12453
J. Phys. Chem. C 2019, 123, 11539−11545

(39) González-Arellano, C.; Abad, A.; Corma, A.; García, H.; Iglesias, M.; Sánchez, F. Catalysis by Gold(I) and Gold(III): A Parallelism between Homo- and Heterogeneous Catalysts for Copper-Free Sonogashira Cross-Coupling Reactions. *Angew. Chem. Int. Ed.* **2007**, *46*, 1536−1538.
(40) Linic, S.; Aslam, U.; Boerigter, C.; Morabito, M. Photochemical Transformations on Plasmonic Metal Nanoparticles. *Nat. Mater.* **2015**, *14*, 567−576.
(41) Linic, S.; Christopher, P.; Ingram, D. B. Plasmonic-Metal Nanostructures for Efficient Conversion of Solar to Chemical Energy. *Nat. Mater.* **2011**, *10*, 911−921.
(42) Marimuthu, A.; Zhang, J.; Linic, S. Tuning Selectivity in Propylene Epoxidation by Plasmon Mediated Photo-Switching of Cu Oxidation State. *Science* **2013**, *339*, 1590−1593.
(43) Marimuthu, A.; Christopher, P.; Linic, S. Design of Plasmonic Platforms for Selective Molecular Sensing Based on Surface-Enhanced Raman Spectroscopy. *J. Phys. Chem. C* **2012**, *116*, 9824−9829.
(44) Willets, K. A.; Van Duyne, R. P. Localized Surface Plasmon Resonance Spectroscopy and Sensing. *Annu. Rev. Phys. Chem.* **2007**, *58*, 267−297.
(45) See Supplementary Materials for more details.
(46) Sagadevan, A.; Ragupathi, A.; Lin, C.-C.; Hwu, J. R.; Hwang, K. C. Visible-Light Initiated copper(I)-Catalysed Oxidative C−N Coupling of Anilines with Terminal Alkynes: One-Step Synthesis of α-Ketoamides. *Green Chem.* **2015**, *17*, 1113−1119.
(47) Sagadevan, A.; Charpe, V. P.; Hwang, K. C. Copper(I) Chloride Catalysed Room Temperature Csp−Csphomocoupling of Terminal Alkynes Mediated by Visible Light. *Catal. Sci. Technol.* **2016**, *6*, 7688−7692.
(48) Mulvaney, P Surface Plasmon Spectroscopy of Nanosized Metal Particles. *Langmuir* **1996**, *12*, 788−800.
(49) Cheng, Y.; Wang, M.; Borghs, G.; Chen, H. Gold Nanoparticle Dimers for Plasmon Sensing. *Langmuir* **2011**, *27*, 7884−7891.
(50) *Phenylacetylene*. https://webbook.nist.gov/cgi/cbook.cgi?ID=C536743&Mask=400#UV-Vis-Spec (accessed Dec 2, 2017).
(51) Marimuthu, A.; Merritt, J.; Brown, G.; Kuehne-Willmore, J. Strategy to Avoid Catalyst Deactivation in Telescoped Miyaura Borylation/Suzuki Cross-Coupling Reaction. *AIChE Annu. Meet. 2014 Conf. Proc.* Atlanda, GA, USA.
(52) Wei, C. S.; Davies, G. H. M.; Soltani, O.; Albrecht, J.; Gao, Q.; Pathirana, C.; Hsiao, Y.; Tummala, S.; Eastgate, M. D. The Impact of Palladium(II) Reduction Pathways on the Structure and Activity of Palladium(0) Catalysts. *Angew. Chem. Int. Ed.* **2013**, *52*, 5822−5826.
(53) Molander, G. A.; Biolatto, B. Palladium-Catalyzed Suzuki−Miyaura Cross-Coupling Reactions of Potassium Aryl- and Heteroaryltrifluoroborates. *J. Org. Chem.* **2003**, *68*, 4302−4314.
(54) Lumerical Inc. http://www.lumerical.com/tcad-products/fdtd/ (accessed Sep 29, 2016).
(55) Cao, Y.; Manjavacas, A.; Large, N.; Nordlander, P. Electron Energy-Loss Spectroscopy Calculation in Finite-Difference Time-Domain Package. *ACS Photonics* **2015**, *2*, 369−375.
(56) Palik, E. D. *Handbook of Optical Constants of Solids*, 1 edition.; Academic Press: San Diego, Calif., 1997.
(57) Jana, N. R.; Gearheart, L.; Murphy, C. J. Seeding Growth for Size Control of 5−40 Nm Diameter Gold Nanoparticles. *Langmuir* **2001**, *17*, 6782−6786.

DOI: 10.1021/acs.jpcc.8b12453
J. Phys. Chem. C 2019, 123, 11539−11545